Experimental Evaluation of a High Fineness Ratio Body with Drag Brakes

Corey J. Florendo,* Thomas R. Yechout,† Stefan Siegel,‡ and Russell M. Cummings†
U.S. Air Force Academy, Colorado Springs, Colorado 80840
and
Joseph Kealos§
Textron, Inc., Wilmington, Massachusetts 01887

The Advanced Remote Ground Unattended Sensor uses drag brakes to control its terminal velocity during flight. An experimental evaluation of the geometry was performed at Mach numbers between 0.20 and 0.50 with a 61.5% scale model in the U.S. Air Force Academy Subsonic Wind Tunnel. Configurations tested include baseline drag brakes fully deployed, an array of perforated drag brake designs, as well as various other related drag brake design features. Improvements to the baseline design are discussed and an improved configuration is presented. Limited unsteady computations were performed for selected cases using detached-eddy simulation to understand various experimental results. The overall flight characteristics of the Advanced Remote Ground Unattended Sensor were improved, including the elimination of unusual lift trends and the tendency of the vehicle to exhibit coning motion during freefall.

Nomenclature

$B_{i\psi}$	=	test instrument overall bias error
$C_{D\psi}$	=	drag coefficient, $D/q_\infty S\psi$
$C_{L\psi}$	=	lift coefficient, $L/q_\infty S\psi$
$C_{m\psi}$	=	pitch moment coefficient, $m/q_\infty Sd\psi$
$C_{n\psi}$	=	yaw moment coefficient, $n/q_\infty Sd\psi$
$D\psi$	=	drag
$d\psi$	=	reference diameter
$L\psi$	=	lift
$M\psi$	=	Mach number
$m\psi$	=	pitch moment
$n\psi$	=	yaw moment
$P_{i\psi}$	=	test instrument overall precision error
$q\psi$	=	dynamic pressure, $\rho V^2/2$
$S\psi$	=	reference area, $\pi d^2/4$
$U_{i\psi}$	=	test instrument overall uncertainty
$V\psi$	=	velocity
$V_{T\psi}$	=	terminal velocity
$W\psi$	=	weight
$\alpha\psi$	=	angle of attack, deg
$\rho\psi$	=	density
$\phi\psi$	=	roll angle, deg

Subscript

$\infty\leftarrow$	=	freestream condition

Presented as Paper 0666 at the AIAA 44th Aerospace Sciences Meeting, Reno, NV, 9–12 January 2006.

*Second Lieutenant, Department of Aeronautics, U.S. Air Force
†Professor of Aeronautics, Department of Aeronautics. Associate Fellow AIAA.
‡Researcher, Department of Aeronautics, Aeronautics Laboratory. Senior Member AIAA.
§Senior Aerodynamicist, Advanced Missile Systems Department. Member AIAA.

I. Introduction

THE design evolution of a high fineness ratio body with drag brakes is presented, focusing on the wind-tunnel testing that directly contributed to definition of the final design configuration [1]. The flight vehicle described here was called the Advanced Remote Ground Unattended Sensor (ARGUS), and was intended to be deployed from an aircraft. After being dropped from a carrier aircraft, the ARGUS was designed to deploy drag brakes to slow it to a predetermined terminal velocity, follow a ballistic flight trajectory until it was flying vertically, and then penetrate the ground. It was crucial that the ARGUS impact the ground in a near-vertical attitude to meet ground penetration and structural requirements.

Four problems with the vehicle had been identified during initial flight testing. First, the lift characteristics of the ARGUS were found to potentially cause the ARGUS to rise back toward the carrier aircraft and create a hazard. Second, yaw moment excursions were identified that would perturb the ARGUS from a trimmed condition, and third, after such a perturbation, the stabilizing pitch moment of the ARGUS was found to be very limited in restoring the vehicle to a steady trimmed condition. The last two aerodynamic characteristics led to a yaw-roll coupling that caused a coning motion of the vehicle during flight. Finally, the terminal velocity of the initial ARGUS design was found to be approximately 15% lower than the desired terminal velocity of 265 ft/s, which needed to be addressed.

The yaw and pitch moment characteristics had been identified as the probable cause of the coning experienced during the preliminary flight tests. To correct the coning problem, a perforated drag brake design (as an alternative to the initial solid drag brake design) was suggested to reduce asymmetric vortex shedding that was predicted to be occurring behind the solid drag brakes of the initial ARGUS design. The perforated drag brake design was found to significantly improve the performance of ARGUS and have a positive effect on the four problems identified, giving the ARGUS desirable aerodynamic characteristics. A follow-on wind-tunnel investigation was then performed in an attempt to optimize the perforation pattern on the drag brakes. Five perforation patterns were evaluated, including the "baseline" pattern from the initial testing, which led to a final drag brake design. Results from flight test confirmed that the drag brake design mitigated the coning effect that was previously seen and resulted in satisfactory performance. A final wind-tunnel investigation was conducted to establish baseline aerodynamic data for the final design and to investigate the aerodynamic effects of the

addition of a release lanyard system for deployment from a carrier aircraft.

This paper highlights the important results of the wind-tunnel investigations and discusses the design process that went on during test and evaluation. Additional numerical simulations were performed to help answer some of the questions posed by the wind-tunnel and flight tests [2]. The final ARGUS configuration was greatly improved by the collaborative design process that included wind-tunnel and flight testing, as well as numerical simulation.

II. Experimental Methods

The initial full-scale ARGUS geometry (see Fig. 1) is composed of three primary sections: a forebody, an aftbody, which is distinguished by a larger diameter than the forebody, and four drag brakes, which surround the aft body. The area of the aftbody behind the drag brakes is commonly referred to as the "tail cone" of the ARGUS, and this area was a primary focus of the aerodynamic testing of the ARGUS. A 61.5% scale model was fabricated of the ARGUS for use in wind-tunnel testing, with Fig. 2 showing the aftbody of the ARGUS wind-tunnel model used in testing. The scale model ARGUS was mounted on an Able internal force balance, which was then mounted on a sting in the test section of the wind tunnel. The 61.5% scale was chosen to keep wind-tunnel blockage in the test section below 5% based on frontal area; the actual blockage at the highest angle of attack for most testing was under 3%. Data were gathered in the Subsonic Wind Tunnel at the U.S. Air Force Academy, which has a 3×3-ft test section and a maximum Mach number of 0.6. All testing was accomplished between Mach 0.2 and Mach 0.5. Mach 0.5 was chosen due to the fact that the wind tunnel was approaching its operating power limit with the high drag of the ARGUS model, and Mach 0.2 was chosen because it is approximated the desired terminal velocity of the ARGUS. The angle of attack range examined was $-4 \leq \alpha, \beta \leq 20$ deg for most test runs. Because of the fact that the wind tunnel is a closed-loop, single-return tunnel, a small amount of flow angularity was present in the test section. To counter this, a yaw (or beta) offset of 0.3 deg was used in most tests. Data were acquired and reduced on an HP3853 Data Acquisition System using software developed at the U.S. Air Force Academy. At each test point data samples were taken at 100 Hz for 2 s, and those samples were averaged to produce time-averaged data. The final series of tests (Phase 3) investigated the time history of the data to observe any unsteady phenomena.

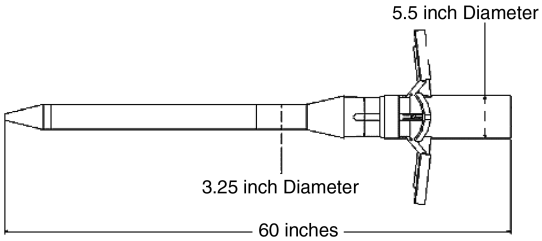

Fig. 1 ARGUS initial design (full-scale).

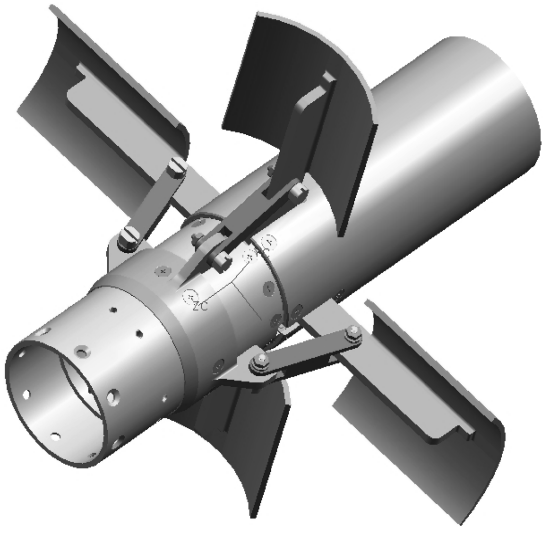

Fig. 2 ARGUS aft body used for phase 1 testing with solid drag brakes.

Table 1 ARGUS coefficient reference dimensions for 61.5% scale model

Testing phase	Reference length	Reference area
Phase 1	2.00 in.	3.142 in.^{2}
Phases 2 and 3	2.154 in.	3.642 in.^{2}

There were four primary aerodynamic coefficients used throughout the ARGUS investigation (the coefficient reference lengths and areas are presented in Table 1). The lift coefficient was examined to ensure that a positive lift-curve slope was present, especially at low angles of attack (where the ARGUS will be released from the carrier aircraft and therefore pose the greatest threat to that aircraft). This positive lift-curve slope ensures that as the ARGUS decreases its angle of attack, its lift also decreases. If a negative lift-curve slope was present, the ARGUS would increase lift as the angle of attack decreased after release, possibly moving ARGUS back toward the carrier aircraft. The second criterion involved the pitch moment and the vehicle's longitudinal static stability. As the angle of attack increased from trim, longitudinal stability required that the ARGUS experience an inherent pitch moment back to the trim condition. Higher stability was indicated by a steeper negative slope of pitch moment as a function of angle of attack. In the third criterion, the yaw moment was examined to ensure yaw excursions were minimized as variations were made in angle of attack. Minimal yaw moment excursions, combined with longitudinal static stability, were predicted to contribute to the mitigation of the coning tendency discussed earlier. Finally, the drag of each ARGUS configuration was examined to determine how closely each design matched the target terminal velocity of 265 ft/s.

The terminal velocity of the ARGUS was calculated using Eq. (1):

$$V_{T\psi} = \sqrt{\frac{2W\psi}{C_D \rho S \psi}} \tag{1}$$

The Reynolds number for the ARGUS configuration in the Subsonic Wind Tunnel was approximately 450,000 (based on reference diameter). The moment reference center was 55% of the body length.

III. Numerical Methods

A computational fluid dynamics (CFD) analysis was performed on a Beowulf cluster located at the U.S. Air Force Academy's Modeling & Simulation Research. Details about the CFD study may be found in [2], but a brief overview of the methods used is presented here.

A. Flow Solver

Solutions for all configurations were computed with the commercial version of Cobalt developed by Cobalt Solutions, LLC. Cobalt solves the unsteady, 3-D, compressible Navier–Stokes equations on a hybrid unstructured grid. Full details of the computational scheme are presented in [3]. The code has several choices of turbulence models, including Spalart–Allmaras (SA), and Menter's Shear Stress Transport (SST) Reynolds-averaged Navier–Stokes (RANS), as well as detached-eddy simulation (DES) versions of SA and SST. All simulations were computed on unstructured meshes with prisms in the boundary layer and tetrahedra elsewhere. The computational meshes were generated with the software packages GridTool [4] and VGRIDns [5].

B. Spalart–Allmaras Turbulence Model

The Spalart–Allmaras [6] one-equation model (SA) solves a single partial differential equation for a working variable $\tilde{\nu}$, which is related to the turbulent viscosity. The differential equation is derived by "using empiricism and arguments of dimensional analysis, Galilean invariance, and selected dependence on the molecular viscosity" [6]. The model has been shown to work well and includes a wall destruction term that reduces the turbulent viscosity in the laminar sublayer.

C. Detached-Eddy Simulation

The DES method was proposed by Spalart et al. [7] and was originally based on the Spalart–Allmaras one-equation RANS turbulence model. DES uses a RANS turbulence model (SA) for attached flow and large-eddy simulation (LES) for separated flow regions. To exhibit both RANS and LES behavior, the model switches into LES mode when the grid is locally refined. DES was implemented in an unstructured grid method by Forsythe et al. [8]. DES was shown to work very well for missile base flows by Forsythe et al [9].

IV. Experimental Uncertainty

An uncertainty analysis using the AIAA total-systems approach was performed for all testing [10]. Both bias error and precision error contributed to the overall uncertainty. A root-sum-square method was used to determine the overall uncertainty, as shown in Eq. (2) [11]:

$$U_{i\psi} = \sqrt{B_{i\psi}^2 + P_{i\psi}^2} \tag{2}$$

To minimize bias error, the test equipment was calibrated to the highest standards possible before each phase of testing. During this calibration, bias error influence coefficients were determined for each specific piece of test equipment. The Able force balance had 10 total bias error coefficients, one for the positive and negative direction of each measured force (two normal forces, two side forces, one axial force). The calibration of the test equipment reduced the contribution of bias error to less than 10% of the overall error. The precision error, which is a function of the standard deviation of the 200 data samples taken at each data point (taken at 100 Hz for 2 s), was much more difficult to minimize. This was due primarily to oscillations that were apparent in the time-history data recorded during Phase 3 testing. These oscillations resulted from low-amplitude vibration of the ARGUS model and increased the standard deviation of the data samples collected during the 2-s intervals, which thereby increased the precision error and thus the overall uncertainty of the data during all three phases of testing. The yaw moment coefficient had the greatest percent uncertainty, mainly because the yaw moments experienced by the ARGUS were of very small magnitude, especially in comparison to the pitch moment coefficient. This small magnitude resulted in a large percentage of uncertainty in the results, even with small absolute values of uncertainty. However, because the time-history data showed that large standard deviations in the data were from oscillations around the average value reported in testing, the uncertainty calculated for this testing can be considered worst case. Table 2 presents the average uncertainty for each calculated coefficient through all phases of testing.

Table 2 Average uncertainty in calculated ARGUS coefficients

Mach	$C_{L\psi}$	C_n	C_m	$C_{D\psi}$
0.2	±14%	±81%	±1%	±2%
0.5	±16%	±78%	±2%	±1%

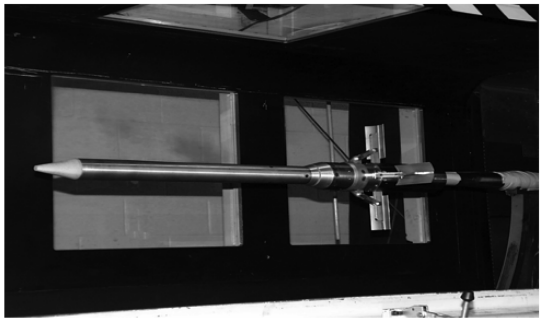

Fig. 3 Phase 1 ARGUS design mounted in U.S. Air Force Academy Subsonic Wind Tunnel.

V. Experimental Results

A. Phase 1 Wind-Tunnel Testing

Phase 1 testing established baseline aerodynamic data for the initial ARGUS design, which are presented in Figs. 1 and 3, and which included solid drag brakes and drag brakes with perforations (the purpose of the perforations will be discussed shortly). Results from this initial testing of the solid drag brakes showed that ARGUS had undesirable aerodynamic characteristics in several areas. First, ARGUS exhibited a negative lift-curve slope, especially at low angles of attack, which can be seen in Fig. 4 for the baseline (solid) drag brake design. The initial offset in lift at low angles of attack was

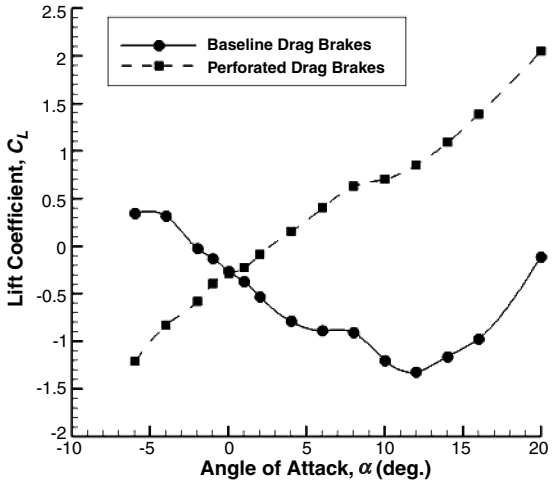

Fig. 4 Lift coefficient as a function of angle of attack for Phase 1 ARGUS design.

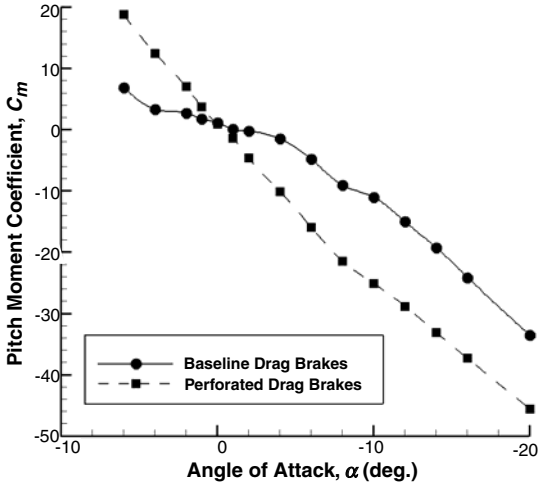

Fig. 5 Pitch moment coefficient as a function of angle of attack for Phase 1 ARGUS design.

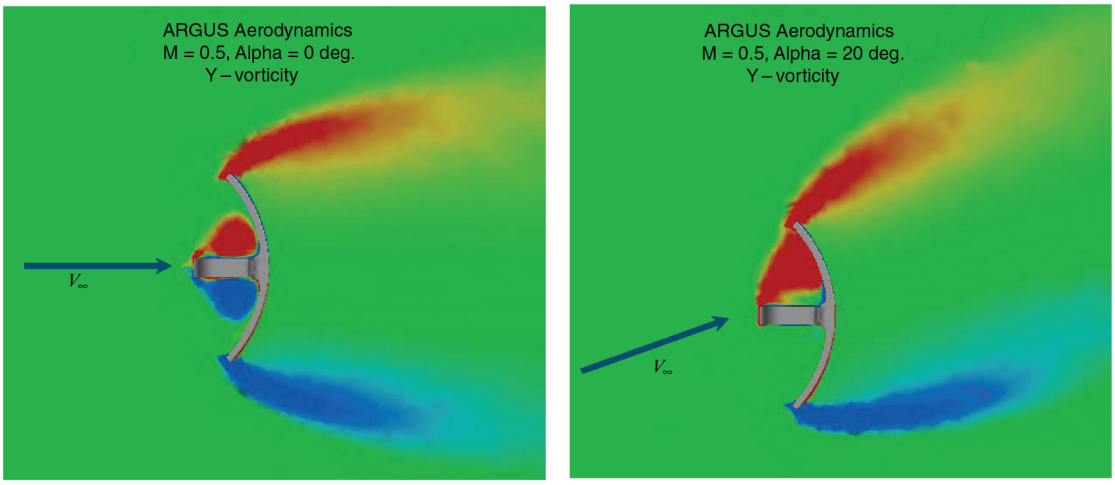

a) $\alpha = 0$ degrees **b) $\alpha = 20$ degrees**

Fig. 6 Computed vorticity contours on drag brakes for $M = 0.5$, $\phi \neq 0$.

also seen in the pitch moment (as seen in Fig. 5) where a positive (nose-up) pitch moment at 0 deg angle of attack was also present. These traits, which were apparent in all phases of testing, were attributed to a slight nose-down attitude of the ARGUS model while mounted on the test sting at 0 deg angle of attack. Because the same forebody was used during all phases of testing and only increased in size as necessary, a slight flaw in the original fabrication likely caused this abnormality.

The offsets in the lift and pitch moment at 0 deg angle of attack do not explain the continuing negative lift trend as angle of attack increases, as shown in Fig. 4. As discussed earlier, this negative lift-curve slope could potentially cause the ARGUS to rise towards the carrier aircraft upon release. Additionally, the data showed that ARGUS had near-neutral longitudinal stability near the trim angle of attack of 0 deg, as seen in Fig. 5. Perforations were added to the drag brakes to help alleviate this behavior; perforations have long been known to help in reducing unsteadiness on surfaces such as flaps and speed brakes [12]. Although the baseline drag brakes exhibited the negative lift behavior, the brakes with perforations had positive lift at positive angles of attack. The pitch moment trends near 0 deg angle of attack were also improved with the perforated drag brakes.

Although the wind-tunnel results could not address the reason for the negative lift behavior, further investigation with CFD showed the basic causes. The numerical simulation was able to give force breakdown information for the vehicle (the lift due to the fuselage and the lift due to the drag brakes), which was very informative [2]. Although the fuselage results look fairly normal for such a configuration, the drag brakes exhibit increasingly negative lift with increasing angle of attack. Flow visualization shed light on the situation, as the curved drag brake extension arm (see Fig. 2) created a region of low pressure due to flow separation on the upper surface of the fin at $\alpha \neq 20$ deg. Figure 6 shows y-vorticity contours in the vicinity of the drag brake and shows flow separation over the support arm, which extends over most of the upper half of the brake. Therefore, the lower surface of the brake has attached flow, but the curved nature of the brake creates a negative lift coefficient, whereas the upper surface of the brake has separated flow and does not counter the force or moment created on the lower surface. When perforations were added to the drag brakes, the lower surface of the brake had reduced area (and therefore less negative lift). The separated flow on the upper surface also was found to flow through the perforations and reduce the adverse lift characteristics.

Yaw moment excursions were found to be large with variation in angle of attack on the baseline drag brakes, as seen in Fig. 7. In addition to these yaw moment characteristics, the near-neutral longitudinal stability was a probable cause of the coning experienced in flight tests. It was concluded that the flow interaction between the drag brakes and the aft body of the ARGUS caused these adverse aerodynamic characteristics. Specifically, there was likely asymmetric vortex shedding occurring off of the drag brakes that was impacting the aft section of the main body, causing poor lift and longitudinal stability characteristics, as well as yaw moment

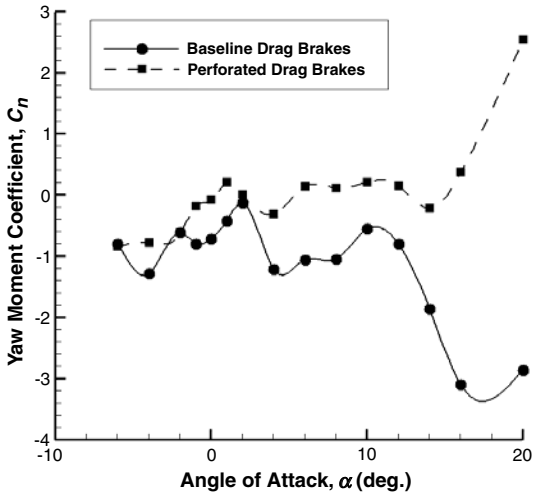

Fig. 7 Yaw moment coefficient as a function of angle of attack for Phase 1 ARGUS design

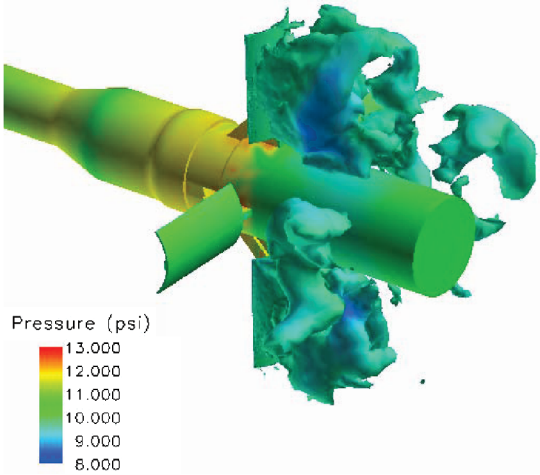

Fig. 8 Detached-eddy simulation showing flowfield around aft section of the ARGUS for the baseline drag brakes.

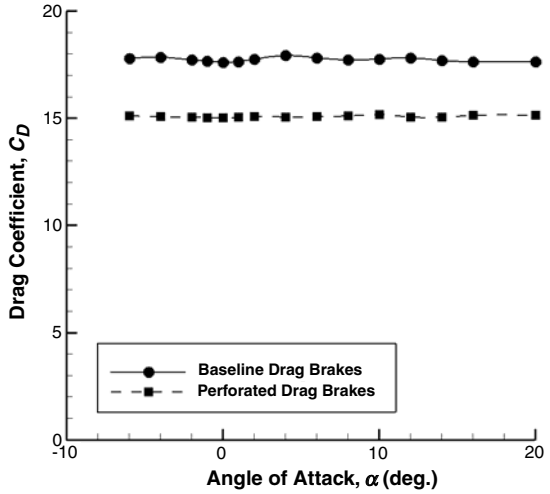

Fig. 9 Drag coefficient as a function of angle of attack for Phase 1 ARGUS design.

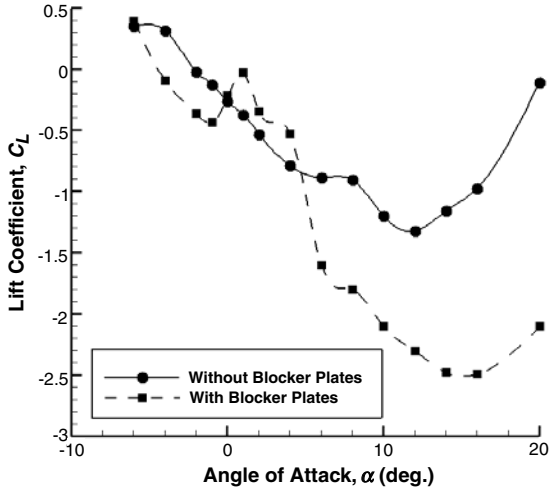

Fig. 11 Lift coefficient as a function of angle of attack for Phase 1 ARGUS design.

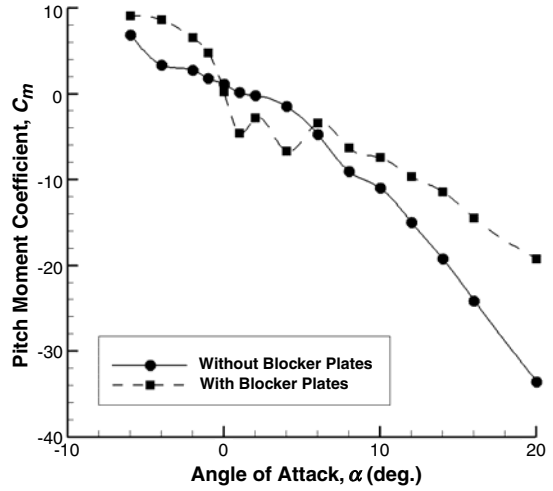

Fig. 12 Pitching moment coefficient as a function of angle of attack for Phase 1 ARGUS design.

excursions. This hypothesis was affirmed by the CFD results, presented in Fig. 8, in which DES was used to verify the strong vortex shedding off the solid drag brakes [2].

Figure 9 presents the drag coefficients obtained for the Phase 1 ARGUS design. The goal for terminal velocity of the ARGUS was initially set at 265 ft/s. The drag coefficient at 0 deg angle of attack can be seen to be approximately 15 for the perforated drag brake design and approximately 17.5 for the solid drag brake design. The weight of the ARGUS was assumed to be 65 lb, the design point during this phase in testing. Using the method in Eq. (1), the perforated drag brakes were found to have a terminal velocity of 260 ft/s, whereas the increased drag of the solid drag brakes lowered the terminal velocity to 230 ft/s. Therefore, in addition to the gains described earlier, perforating the drag brakes also allowed for the ARGUS to achieve a terminal velocity closer to the prescribed goal. Therefore, at the end of phase 1 testing, the ARGUS was found to have suitable aerodynamic characteristics in all areas of interest if the perforated drag brakes were used.

The final effort during phase 1 was aimed at mitigating the adverse aerodynamic characteristics seen in initial testing by using "blocker plates" to remove the space between the drag brakes and the ARGUS main body (see Fig. 10) [13]. It was established in previous testing that the ARGUS had desirable aerodynamic characteristics without the drag brakes deployed, so the blocker plates were used in an attempt to correct the problems that became apparent with the addition of the drag brakes.

The addition of the blocker plates, which eliminated the airflow in the gap between the drag brakes and the aft body, worsened all of the negative trends observed before this modification. Figure 11 shows that the lift-curve slope was even more negative with the blocker plates, whereas Fig. 12 shows that neutral longitudinal stability or instability was exhibited near 0 deg angle of attack.

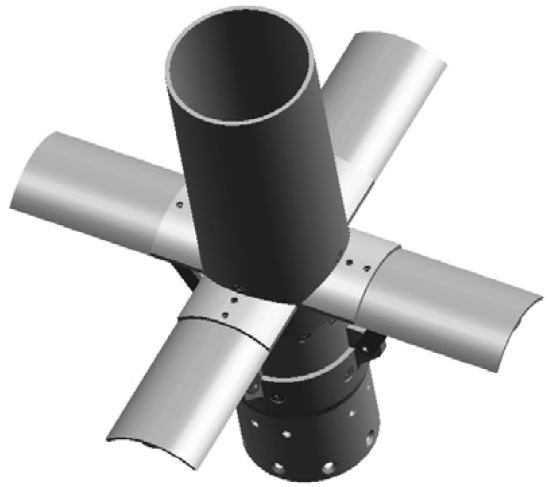

Fig. 10 ARGUS aftbody with blocker plates installed below drag brakes.

The greatest improvements in the aerodynamic characteristics were obtained from adding perforations to the drag brakes, as can be seen in the comparisons in Figs. 4 and 5 with Figs. 11 and 12. Adding perforations created a nearly linear positive lift-curve slope, gave very stable longitudinal stability about the trim angle of attack of 0 deg, and reduced the magnitude of the yaw moment excursions. This formed the basis for the next phase of testing to determine the optimum perforation design for the drag brakes.

B. Phase 2 Wind-Tunnel Testing

It was decided after examination of the results of Phase 1 testing to incorporate drag brake perforations into the working ARGUS design to mitigate the asymmetric vortex shedding from the drag brakes. The focus of the Phase 2 testing was to optimize the perforation pattern of the drag brakes. The drag brake perforation pattern used in Phase 1 was defined as the baseline design and variations were made to the size of the holes and their alignment in an attempt to further improve the aerodynamic characteristics of the ARGUS. Additionally, a "mixed" configuration of large and small perforations was also tested. The five drag brake configurations evaluated are presented in Fig. 13. This investigation was one of the few documented cases in which the effects of perforation patterns on drag-inducing devices

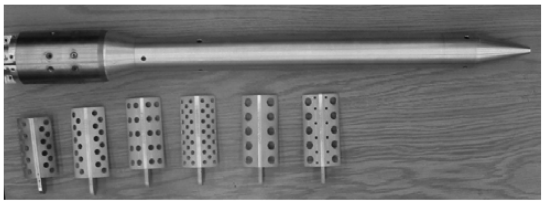

Fig. 13 Baseline, aligned, small, large, and mixed perforation drag brake configurations with ARGUS fuselage.

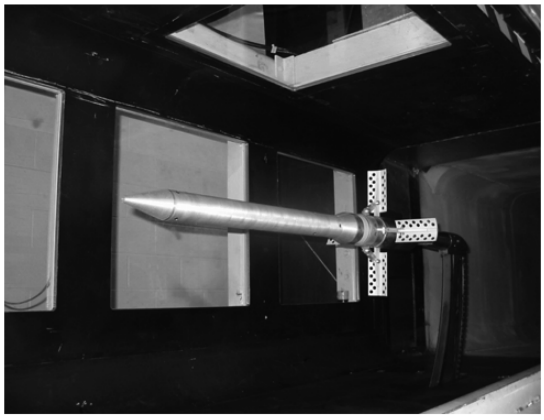

Fig. 14 Phase 2 ARGUS model mounted in U.S. Air Force Academy Subsonic Wind Tunnel.

has been examined. Though the perforation configurations were varied, the ratio of the area of the holes to the area of the drag brake was kept constant throughout testing. Additionally, the weight increased to 80 lb and the size of the forebody was increased to 3.5 in.ψ(from 3.25 in.ψ(full-scale) to accommodate internal component growth, so the Phase 2 testing also provided baseline data for the new, larger ARGUS design. Figure 14 shows the Phase 2 ARGUS design with the baseline perforated drag brakes mounted on the test sting in the wind tunnel.

Figure 15 shows that the lift characteristics of the baseline and mixed configuration perforated drag brake designs were comparable and did not exhibit any major undesirable characteristics. The large-hole configuration provided a steeper lift-curve slope and therefore more desirable lift characteristics, whereas the aligned holes and small holes exhibited undesirable lift curves. Figure 16 shows that all drag brake configurations exhibited longitudinal static stability, with the baseline configuration demonstrating the most stability, and the aligned configuration the worst; however, all of the configurations exhibited acceptable pitch moment characteristics.

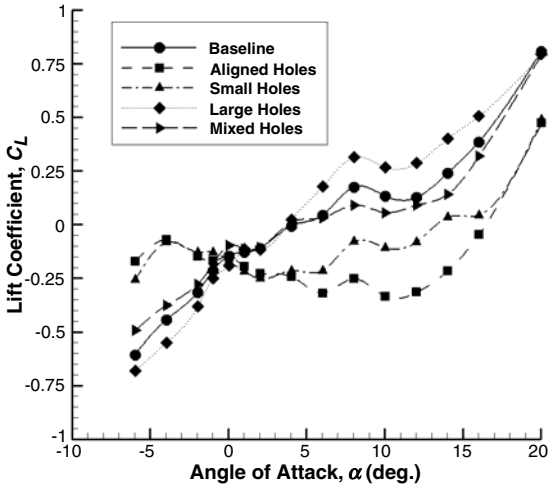

Fig. 15 ARGUS lift coefficient vs angle of attack for various perforation designs.

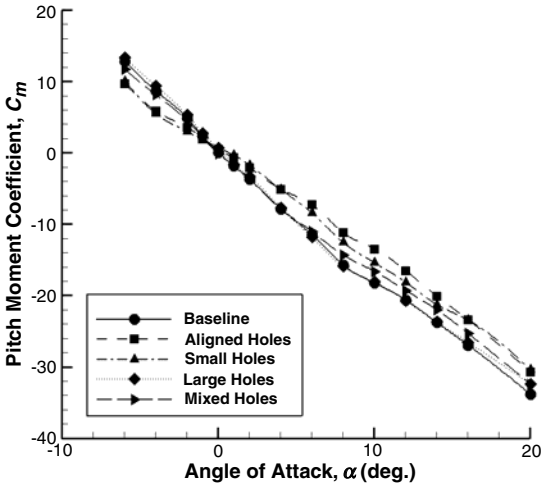

Fig. 16 ARGUS pitch moment coefficient vs angle of attack for various perforation designs.

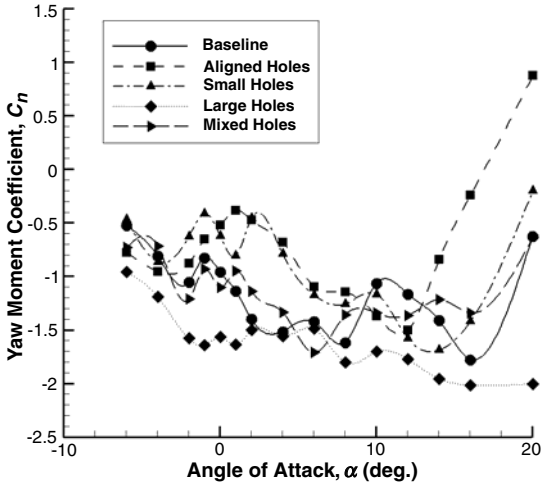

Fig. 17 ARGUS yaw moment coefficient vs angle of attack for various perforation designs.

Despite the fact that the large holes provided the most desirable lift characteristics, Fig. 17 shows that the large holes also provided the least desirable yaw moment characteristics, in that they exhibited large yaw moment excursions that grew in intensity with increasing angle of attack. The baseline and mixed configuration again produced similar results, whereas the aligned and small holes, providing the least desirable lift characteristics, interestingly exhibited the smallest yaw moment excursions.

The drag coefficient for each configuration is presented in Fig. 18. Using Eq. (1), the baseline configuration was found to have the lowest terminal velocity of 256 ft/s, and the mixed configuration was the highest at 260 ft/s. The slight variation in the terminal velocity between the drag brake perforation designs was attributed to the fact that only the perforation pattern was changed on the drag brakes, whereas the hole/area ratio was kept constant. With the Phase 2 ARGUS configuration and perforated drag brake designs, the terminal velocity projections were close to the desired target terminal velocity. This was due to an effort to match the size and drag of the new drag brakes to the larger, heavier ARGUS design [14]. The positive effect of the drag brake perforations can also be seen in Fig. 19, which is the DES simulation for the ARGUS with the perforations added to the drag brakes at Mach 0.5 and 0 deg angle of attack [2]. Comparing Fig. 8 with Fig. 19, it can be seen that the addition of the perforations mitigated the large vortices that were occurring behind the drag brakes of the ARGUS, allowing for improved (and more steady) aerodynamic performance.

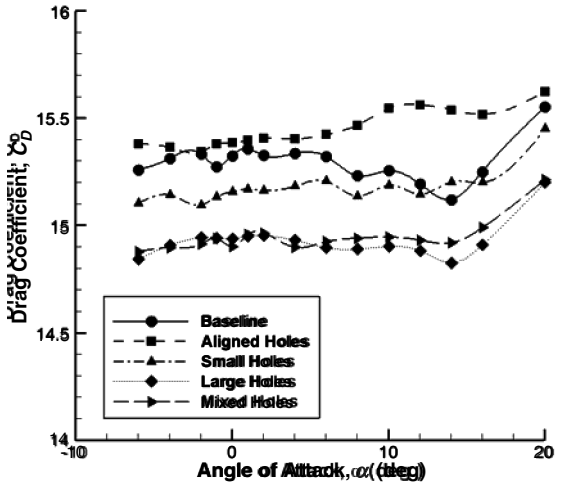

Fig. 18 ARGUS drag coefficient vs angle of attack for various perforation designs (note decreased scale for ease of differentiation).

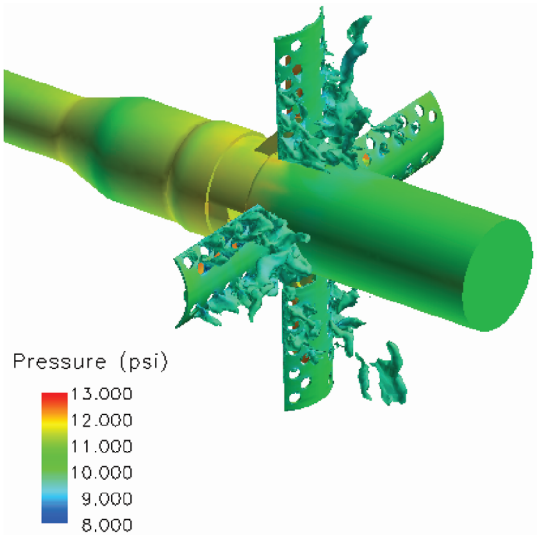

Fig. 19 CFD simulation image showing flowfield around aft section of the Phase 2 ARGUS design.

This testing was able to quantify the effects of the differing perforation patterns on the aerodynamic characteristics of the ARGUS. As a result of the testing, either the baseline or the mixed perforations were found to be suitable for the ARGUS design. The baseline perforation design was chosen based on producibility considerations and successful drop tests with this configuration, which occurred concurrently with the Phase 2 testing. This baseline configuration produced suitable aerodynamic characteristics in all areas of interest.

C. Unsteady Aerodynamics Results for the Lanyard System

The final stage of wind-tunnel testing, Phase 3, had multiple objectives: 1) determine the impact of varying subsonic Mach numbers on the aerodynamics, and 2) determine the unsteady aerodynamics of a lanyard system, shown in Fig. 20. The length of the full-scale design was increased 2 in. in the aft section to allow room for electronics, and the drag brakes were located 1 in. further aft on the tail can. These geometric modifications did not appreciably alter the dynamics of the vehicle; details can be found in [13]. The lanyard was used to stow the drag brakes during carriage aboard an aircraft, deploy the drag brakes upon release, and then remain attached to ARGUS during descent. This testing was accomplished using not only the time-averaged data that had been used previously, but also with time-history data. Thus, the final objective was to identify any unsteady phenomena not seen previously.

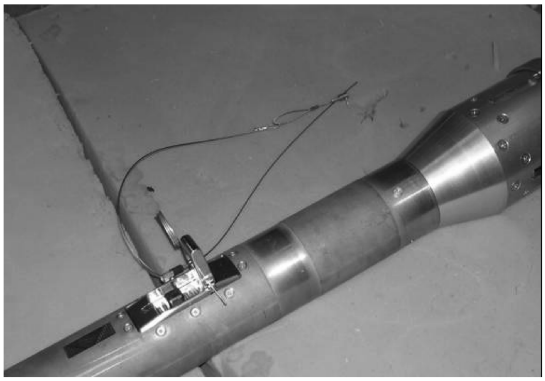

Fig. 20 Lanyard release system on Phase 3 ARGUS model.

Before this, experimental results have only been presented at Mach 0.2, as results at higher Mach numbers closely mirrored the results from Mach 0.2. However, the Phase 3 ARGUS configuration was run at $M_\infty = 0.2, 0.3, 0.4$, and 0.5 to determine if any significant Mach effects were present. Although increased Mach number decreased the lift-curve slope and led to slightly less longitudinal static stability, the lift and pitch moment characteristics of the ARGUS were not appreciable different at any Mach number tested. Also, increased Mach number created yaw moment excursions that were greater than at Mach 0.2; however, the larger excursions were not of sufficient magnitude to constitute unusual characteristics. The drag coefficients showed the expected behavior, namely, that the ARGUS drag coefficients increased at higher Mach numbers; however, it should be pointed out that the drag coefficient at Mach 0.2 was the value used in the calculation of the terminal velocity. The terminal velocity for the Phase 3 ARGUS design was calculated to be 258 ft/s. This small increase in terminal velocity over Phase 2 with the baseline perforated drag brakes was attributed to the 1 in. further aft location of the drag brakes on the aft body.

Testing revealed that the addition of the lanyard and the larger aft section did not degrade any of the aerodynamic characteristics seen in previous testing. A time-history investigation of the Phase 3 test data showed that oscillations were apparent in all of the coefficients calculated. These oscillations were at approximately the same frequency for the drag, pitch moment, side force, and yaw moment coefficients, and at approximately twice that frequency for the lift coefficient. These oscillations are likely a result of the ARGUS model support configuration, composed of the ARGUS model, force balance, and the test sting. The oscillations did not appear to increase or decrease in magnitude for the 2-s period over which the data were collected.

VI. Conclusions

Wind-tunnel and CFD efforts at the U.S. Air Force Academy were essential to development of the final ARGUS design. There were three major conclusions reached during research. During Phase 1, perforated drag brakes significantly improved the aerodynamic stability by mitigating the effects of asymmetric vortex shedding. During Phase 2, the baseline and mixed perforated drag brake designs created optimum aerodynamic characteristics, but the original perforated design was retained due to its overall characteristics. During Phase 3, the addition of the lanyard system did not degrade the overall aerodynamic characteristics of the ARGUS, and time-history data showed that constant-frequency oscillations occurred during testing but did not provide performance concerns. Only minor Mach number effects were seen between $M_\infty = 0.2$ and $M_\infty = 0.5$. As a result of increased weight and a shift in the location of the drag brakes, the Phase 3 configuration was projected to produce a terminal velocity close to the target, thus fulfilling all aerodynamic requirements for the ARGUS.

As a result of the testing, two recommendations were made. First, additional flow visualization methods or CFD analysis is recommended to better understand the complex flow occurring

behind the drag brakes that were the primary cause of the initial adverse aerodynamic characteristics. Second, flight validation of the various experimental and computational results shown here would provide needed insight into our ability to correctly predict and understand these types of drag brakes at flight Reynolds numbers.

Acknowledgments

The authors wish to thank the U.S. Air Force Academy Department of Aeronautics for their support of this wind-tunnel investigation. This support included the use of test facilities, computer clusters, and machine fabrication shops. In addition, Lt. Colonel David Wetlesen of the Department of Aeronautics was instrumental in serving as overall program coordinator. Also, Textron, Inc., was invaluable in providing the overall design lead for ARGUS configurations, fabrication of the model, and guidance on specific test emphasis items.

References

[1] Florendo, C. J., Yechout, T. R., Siegel, S., Cummings, R. M., and Kealos, J. J., "Experimental Evaluation of a High Fineness Ratio Body with Drag Brakes," AIAA Paper 2006-0666, Jan. 2006.

[2] Cummings, R. M., Divine, J. A., Yechout, T. R., Wetlesen, D. C., and Kealos, J. J., "Numerical Evaluation of the Flowfield for a High Fineness Ratio Body with Drag Brakes," AIAA Paper 2006-0668, Jan. 2006.

[3] Strang, W. Z., Tomaro, R. F., and Grismer, M., "Unstructured Euler/ Navier-Stokes Flow Solver," AIAA Paper 99-0786, Jan. 1999.

[4] Samareh, J., "Gridtool: A Surface Modeling and Grid Generation Tool," *Proceedings of the Workshop on Surface Modeling, Grid Generation, and Related Issues in CFD Solution*, CP-3291, NASA, May 1995, pp. 821–831.

[5] Pirzadeh, S., "Progress Toward a User-Oriented Unstructured Viscous Grid Generator," AIAA Paper 96-0031, Jan. 1996.

[6] Spalart, P. R., and Allmaras, S. R., "A One Equation Turbulence Model for Aerodynamic Flows," *La Recherche Aerospatiale: Bulletin Bimestriel de l'Office National d'Etudes et de Recherches Aerospatiales*, Vol. 1, 1994, p. 5.

[7] Spalart, P. R., Jou, W-H., Strelets, M., and Allmaras, S. R., "Comments on the Feasibility of LES for Wings, and on a Hybrid RANS/LES Approach," *Advances in DNS/LES, 1st AFOSR International Conference on DNS/LES*, Greyden Press, Columbus, OH, Aug. 1997.

[8] Forsythe, J. R., Hoffmann, K. A., and Dieteker, F. F., "Detached-Eddy Simulation of a Supersonic Axisymmetric Base Flow with an Unstructured Flow Solver," AIAA Paper 2000-2410, June 2000.

[9] Forsythe, J. R., Hoffmann, K. A., Cummings, R. M., and Squires, K. D., "Detached-Eddy Simulations with Compressibility Corrections Applied to a Supersonic Axisymmetric Base Flow," *Journal of Fluids Engineering*, Vol. 124, No. 4, 2002, pp. 911–923.

[10] DeLoach, D. (ed.), "Assessment of Experimental Uncertainty with Application to Wind-Tunnel Testing," AIAA Standard S-071A-1999, 1999.

[11] Schneider, J., Searcy, J., and Yechout, T., "Investigation and Optimization of NASA Orbital Space Plane Designs," U.S. Air Force Academy Department of Aeronautics, DFAN TR 04-03, 2004.

[12] Turner, T. R., "Wind-Tunnel Investigation of Perforated Split Flaps for Use as Dive Brakes on a Rectangular NACA 23012 Airfoil," NACA WR-L-445, July 1941.

[13] Swierzbin, T., Hellinger, D., Guthmann, C., Yechout, T. R., and Wetlesen, D., "A Wind Tunnel Evaluation of Advanced Remote Ground Unattended Sensor (ARGUS) Configurations," U.S. Air Force Academy Department of Aeronautics, DFAN TR 04-01, 2004.

[14] Florendo, C., Gilbert, J., and Yechout, T., "A Wind Tunnel Evaluation of Perforated Drag Brake Designs for the Advanced Remote Ground Unattended Sensor (ARGUS)," U.S. Air Force Academy Department of Aeronautics, DFAN TR 04-04, 2004.

P. Weinacht
Associate Editor